J. Fluid Mech. (1982), *vol.* 116, *pp.* 507–530
Printed in Great Britain

Quadrupoles in potential flow: two model problems

By H. W. BLACKBURN

Cambridge University Engineering Department,
Trumpington Street, Cambridge CB2 1PZ, U.K.

(Received 1 October 1979 and in revised form 24 July 1981)

The Ffowcs Williams–Hawkings formulation of the sources of the acoustic analogy is examined by reference to two compressible inviscid flows whose density and velocity fields are known exactly. The purpose of this exercise is to generate some feel for the importance of the various source terms in determining the sound of moving surfaces with shocks, and to help quantify the errors involved in approximating those sources. Practical applications of the theory involve flows that cannot be known exactly and the errors of approximation cannot be checked directly. Progress must start with simple cases, and these model problems represent a first move. The flows considered are the one-dimensional flow caused by a plane boundary impulsively accelerated into a fluid, and the two-dimensional flow due to a wedge moving supersonically and supporting a plane attached shock.

For each of these flows, a system of analogous acoustic sources is developed, the fields of which, when superposed, produce a density field (an acoustic field) identical with that of the original flow. The acoustic fields generated by the component source terms are calculated and compared. This suggests that the volume quadrupoles of potential flow play only a minor role as sound generators. When properly viewed the field is generated entirely on the bounding surfaces of the flow. A general argument shows that volume quadrupoles in steady rectilinear motion only influence the sound field through propagation effects.

1. Introduction

There is much current research on high-speed surface-induced noise such as that generated by helicopter rotors, fans, and unducted propellers. These devices operate at speeds extending to supersonic and produce undesirably high sound levels.

Sixty years ago Lynam & Webb (1920) conducted the first experiments on high-speed rotor noise. At that time there was no theoretical framework in which to interpret their observations, and their results on the intense directional noise radiated by static propellers operating with supersonic tip speeds prompted the subjects' first theoretical analysis by Bryan & Lamb (1920). However, this analysis concerned an acoustic model whose simplicity allowed only a qualitative agreement between theory and experiment. Even today the sound-generation mechanisms remain imperfectly understood.

Gutin (1940), in an analysis of propeller noise that was later extended by Garrick & Watkins (1954), assumed that the sound was generated by the steady rotating thrust and drag forces exerted by the blade on the air. Though this was a marked improvement on past theories, their predictions for the harmonic levels of the field failed to

agree with observations on rotors whose tip speeds extended from high subsonic to supersonic and their theoretical predictions were particularly inaccurate for the high-frequency parts of the spectrum.

Adapting the acoustic analogy devised by Lighthill (1952), Ffowcs Williams & Hawkings (1969) have determined a system of acoustic sources that will create density variations in a stationary unbounded uniform acoustic medium identical to those density variations occurring in a real fluid in the presence of moving boundaries. The source system for the acoustic medium involves dipole and monopole sources distributed on surfaces whose shape and disposition are identical to the boundaries of the real fluid, and quadrupole sources distributed throughout the fluid. The acoustic analogy and its extensions due to Curle (1955) and Ffowcs Williams & Hawkings are based solely on the equations of continuity and momentum conservation. Unlike previous theories in which the sources are assumed to be known, theirs is a formal analogy in which exact conservation relations are manipulated into an inhomogeneous wave equation posing a complicated nonlinear diffraction problem; the sources are themselves functions of the field strength.

This version of the acoustic analogy has been the basis for several computational researchers on the noise of helicopters (Farassat 1975; Yu & Schmitz 1980), but the computed results are not entirely satisfactory. Nor are the results of experiments with rotors completely consistent. Boxwell, Yu & Schmitz (1978) report major discrepancies between full-scale ground, full-scale wind-tunnel, model wind-tunnel, and full-scale flight measurements of helicopter blade slap, a directional impulsive sound radiated by high-speed rotors. Computer models of these phenomena tend to be inaccurate at tip speeds near and above sonic.

The difficulties of computer modelling are that it is not known to what extent the analogous sources can be reliably simplified by either discarding some of the source terms or approximating the source strengths, and at what level of geometric and computational sophistication the calculations should be performed. The errors of the methods employed have not yet been quantified, and it is extremely difficult to do so.

It might therefore be worthwhile to examine the acoustic analogy in the context of flow fields for which exact results for the various source terms are known, in order to see how in these cases neglect of some source terms, in particular the quadrupoles, can influence the field. However, in the tractable cases the possibly important effects of source rotation do not occur and so these must remain outside the scope of this discussion.

Calculations by Hanson & Fink (1978) of the contribution of the quadrupole sources to the in-plane sound of a propeller operating at transonic tip speeds indicate that the quadrupole field is extensive but weak, its maximum strength density being 2 % of the source density of equivalent interior quadrupoles, yet their computation of the acoustic field radiated by these sources gives them equal overall importance. This quadrupole field, however, is an important source only in those regions about the rotor moving with speeds between the critical air–foil speed and sonic speed. Yu & Schmitz (1980) have also demonstrated a significant amplitude arising from the quadrupole sources for a helicopter blade with a rotor-tip Mach number in the region of 0·9. In both cases the quadrupole field increases very rapidly with rotor-tip Mach number in the transonic region and, in the work of Hanson & Fink, decays equally rapidly at a Mach number of unity. This paper attempts to determine whether or not this effect is

generally true, and if not, to determine from an exact calculation what the main role of the flow-induced sources is. Evidence is produced that the quadrupoles of potential flow are not so much generators of sound but rather terms needed to position correctly the waves that are essentially generated at the moving surfaces.

2. Acoustic analogy

Ffowcs Williams & Hawkings (1969) posed the acoustic analogy for a fluid bounded by moving surfaces in the form

$$\Box^2\{(\rho-\rho_0)H(f)\} = \frac{\partial^2}{\partial y_i \partial y_j}\{T_{ij}H(f)\} - \frac{\partial}{\partial y_i}\left\{p_{ij}\frac{\partial H}{\partial y_j}\right\} + \frac{\partial}{\partial \tau}\left\{\rho_0 v_i \frac{\partial H}{\partial y_i}\right\}, \tag{2.1}$$

where the function f is defined to be positive in regions occupied by fluid, zero on the bounding surfaces, and negative elsewhere. Equation (2.1) is an exact rearrangement, valid everywhere, of the equations of mass and momentum conservation for a fluid of density ρ, bounded by an impermeable surface moving with speed $\mathbf{v}$. Equation (2.1) represents a complicated nonlinear diffraction problem, but by interpreting it in terms of an acoustic analogy it appears to be more tractable. The field in that analogy is driven by three source terms, quadrupole, dipole, and monopole. The quadrupole is confined to the region external to the surface $f = 0$, whilst the dipole and monopole sources are distributed over that surface.

The exactness of (2.1) guarantees that, taken together, the source terms generate the correct density field; all the effects of sound generation and propagation are accounted for. The major disadvantage of the method is that two of the sources are dependent on the field itself. One aim of this work is to determine how successfully these source strengths may be approximated independent of the field.

When the boundaries of the fluid are rigid and move solenoidally it is convenient to express the integral form of (2.1) in terms of spatial co-ordinates, $\boldsymbol{\eta}$ say, that move with the bounding surfaces. The perturbation $\tilde{\rho} = \rho - \rho_0$ is then given by

$$4\pi c^2 H(f)\tilde{\rho}(\mathbf{x},t) = \frac{\partial^2}{\partial x_i \partial x_j}\int \frac{T_{ij}}{r} H(f)\,\delta(g)\,d\eta^3 d\tau$$
$$-\frac{\partial}{\partial x_i}\int \frac{p_{ij}}{r}\frac{\partial f}{\partial y_j}\delta(f)\,\delta(g)\,d\eta^3 d\tau + \frac{\partial}{\partial t}\int \frac{\rho_0 v_i}{r}\frac{\partial f}{\partial y_i}\delta(f)\,\delta(g)\,d\eta^3 d\tau, \tag{2.2}$$

where $g = \tau - t + r/c$, $r = |\mathbf{x} - \mathbf{y}(\boldsymbol{\eta},\tau)|$, and $f = f(\boldsymbol{\eta})$. The integrands all vanish off the hypersurface $g = 0$, and the latter two integrands also vanish off the hypersurface $f = 0$.

Ffowcs Williams & Hawkings gave several alternative methods for expressing the integrals of (2.2), their methods being based on hypersurface integrals. The integrals can be either projected onto a co-ordinate hyperplane or resolved onto several hyperplanes, or else evaluated directly.

Projection of the integrals onto the hyperplane spanned by the spatial co-ordinates gives the field as

$$4\pi c^2 H(f)\tilde{\rho}(\mathbf{x},t) = \frac{\partial^2}{\partial x_i \partial x_j}\int \left[\frac{T_{ij}}{r|1-M_r|}\right]_{\text{ret}} d\eta^3$$
$$-\frac{\partial}{\partial x_i}\int \left[\frac{p_{ij}n_j}{r|1-M_r|}\right]_{\text{ret}} d\eta^2 + \frac{\partial}{\partial t}\int \left[\frac{\rho_0 v_i n_i}{r|1-M_r|}\right]_{\text{ret}} d\eta^2, \tag{2.3}$$

where M_r is the Mach number at which the source approaches the field position $\mathbf{x}$, and $\mathbf{n}$ is the unit normal of the boundary directed into the fluid. Equation (2.3) can also be obtained from (2.2) by integrating with respect to the source time τ, a method equivalent to projecting along the source-time co-ordinate.

A second projection of the hypersurface $g = 0$ is best illustrated by introducing spherical polar co-ordinates centred at $\mathbf{x}$ to span $\boldsymbol{\eta}$-space. Note that if the source moves, then the point $\mathbf{x}$ moves relative to the $\boldsymbol{\eta}$-frame. The volume element may be written $d\eta^3 = \eta_r^2 \sin\Omega_1 d\eta_r d\Omega_1 d\Omega_2$. This projection is along the η_r direction, onto the co-ordinate hyperplane spanned by Ω_1, Ω_2, and τ. This projection is equivalent to integrating (2.2) with respect to r. The resulting integral expression is

$$4\pi c^2 H(f)\,\tilde{\rho}(\mathbf{x},t) = \frac{\partial^2}{\partial x_i \partial x_j}\int \frac{T_{ij}}{t-r}\,d\Omega\,d\tau - \frac{\partial}{\partial x_i}\int \frac{p_{ij}n_j}{t-\tau}\frac{d\Gamma\,d\tau}{\sin\theta} + \frac{\partial}{\partial t}\int \frac{\rho_0 v_i n_i}{t-\tau}\frac{d\Gamma\,d\tau}{\sin\theta}, \quad (2.4)$$

where $d\Omega$ is a spherical surface element within the fluid. For the surface sources a spatial frame with non-orthogonal co-ordinates r, f, and Γ is used. The directions of f and r make an angle of θ with each other, while Γ is orthogonal to both these directions and lies in the surface $f = 0$. The integrand does not contain the Mach wave singularity which occurs in (2.3) when $|M_r - 1| = 0$. Furthermore, the integration element $d\Gamma/\sin\theta$ remains bounded when θ tends to zero. Consequently the integrand of the τ-integration is discontinuous at times corresponding to the start and finish of the temporal existence of the Γ integration. The following sections utilize (2.3) and (2.4) to evaluate the density variations induced by the individual source terms of two specific compressible fluid flows.

3. One-dimensional flow

The first flow examined is one-dimensional and unsteady. Inviscid compressible fluid, at rest, with density ρ_1 and pressure p_1, occupies the half-space $y_1 > 0$. At time $t = 0$, the plane boundary at $y_1 = 0$ accelerates impulsively into the fluid, attaining a speed V. Simultaneously, a plane shock leaves the boundary and moves ahead of it into the fluid with speed c_s. The shock compresses the fluid that it traverses to a density ρ_2 and pressure p_2, and accelerates it to a speed V. The fluid between the boundary and the shock moves with this uniform speed, the extent of the moving fluid increasing as the shock moves away from the boundary. The flow therefore has an unsteady feature, which cannot be eliminated by changing the frame of reference.

The analysis presented here of the analogous acoustic problem uses (2.3). First the analogous acoustic sources are derived. Application of mass- and momentum-conservation principles to a region containing the shock gives the two relations

$$\rho_1 c_s = \rho_2(c_s - V), \quad (3.1a)$$

$$p_1 = p_2 + \rho_2 V(V - c_s). \quad (3.1b)$$

Introducing $\Delta\rho = \rho_2 - \rho_1$, the surface source $\rho_0 v_n$ has a strength $\Delta\rho(c_s - V)$, the surface stress term p_{ij} the value $\Delta\rho(c_s - V)c_s\delta_{ij}$, and the volume stress T_{ij} takes the form

$$\Delta\rho(c_s V\delta_{i1}\delta_{j1} + (c_s^2 - c^2 - c_s V)\delta_{ij}). \quad (3.2)$$

The $\boldsymbol{\eta}$-co-ordinate frame is chosen to move steadily relative to the undisturbed fluid so that the moving boundary coincides with the plane $\eta_1 = 0$ for $\tau > 0$. The $\mathbf{y}$- and

$\boldsymbol{\eta}$-co-ordinates are then related by $\mathbf{y} = \boldsymbol{\eta} + c\mathbf{M}\tau$, where $(V, 0, 0) = (cM, 0, 0)$ is the $\boldsymbol{\eta}$-frame velocity relative to the $\mathbf{y}$-frame.

Denoting with square brackets the retarded-time value of a function defined in $\boldsymbol{\eta}$-space, we have $[r] = |\mathbf{x} - [\mathbf{y}]|$, and writing $\mathbf{z} = \mathbf{x} - \boldsymbol{\eta} - \mathbf{V}t$ gives

$$[\mathbf{r}] = \mathbf{z} + \mathbf{M}[r]. \tag{3.3}$$

The results

$$[r(1 - M_r)] = -\mathbf{z} \,.\, \mathbf{M} + [r](1 - M^2), \tag{3.4a}$$

$$[r] = \frac{\mathbf{z} \,.\, \mathbf{M} \pm \{(\mathbf{z} \,.\, \mathbf{M})^2 + (1 - M^2) z^2\}^{\frac{1}{2}}}{1 - M^2} \tag{3.4b}$$

follow, allowing the denominator of the integrands of (2.3) to be expressed as functions of $\boldsymbol{\eta}$, that is

$$\begin{aligned}[r|1 - M_r|] &= +\{(\mathbf{z} \,.\, \mathbf{M})^2 + z^2(1 - M^2)\}^{\frac{1}{2}} \\ &= +\{(\eta_1 - x_1 + Vt)^2 + (1 - M^2)\,((\eta_2 - x_2)^2 + (\eta_3 - x_3)^2)\}^{\frac{1}{2}}.\end{aligned} \tag{3.5}$$

We consider first the volume integral of (2.3). The surface integrals are appreciably easier to evaluate in the light of this integral. Using (3.5) in (2.3) gives

$$\int \left[\frac{T_{ij} H(f)}{r|1 - M_r|}\right]_{\text{ret}} d\eta^3 = \int \frac{[T_{ij} H(f)]\, d\eta^3}{\{(\eta_1 - x_1 + Vt)^2 + (1 - M^2)\,((\eta_2 - x_2)^2 + (\eta_3 - x_3)^2)\}^{\frac{1}{2}}}. \tag{3.6}$$

The limits of integration require careful evaluation, for the numerator is to be taken at its retarded time value and the volume stress is unsteady in the $\boldsymbol{\eta}$-frame. The stress can be written as

$$T_{ij} H(\eta_1)\, H((c_s - V)\tau - \eta_1)),$$

showing that the stress is non-zero in the time-dependent region

$$0 < \eta_1 < (c_s - V)\tau. \tag{3.7}$$

To radiate to $(\mathbf{x}, t)$, the point of emission $(\boldsymbol{\eta}, \tau)$ must satisfy

$$|\mathbf{x} - \boldsymbol{\eta} + Vt| = c(t - \tau) \quad (\tau < t). \tag{3.8}$$

If $x_1 < -ct$ or $c_s t < x_1$, no real τ can satisfy (3.7) and (3.8), so the integration region is null and the source does not radiate to $(\mathbf{x}, t)$.

If $-ct < x_1 < c_s t$, the region of integration takes one of two possible shapes depending on whether the boundary moves subsonically or supersonically. When it moves subsonically, the region that radiates to $(\mathbf{x}, t)$ is the interior of the ellipsoid of revolution

$$\frac{\{\eta_1 - (c_s - V)\,(c_s x_1 - c^2 t)/(c_s^2 - c^2)\}^2}{\{c(c_s - V)\,(c_s t - x_1)/(c_s^2 - c^2)\}^2} + \frac{\{\eta_2 - x_2\}^2 + \{\eta_3 - x_3\}^2}{c^2 (c_s t - x_1)^2/(c_s^2 - c^2)} = 1, \tag{3.9}$$

that lies in the half-space $\eta_1 > 0$, see figure 1 (*a*). The ellipsoid lies within the region

$$\eta_L = \frac{(c_s - V)\,(x_1 - ct)}{c_s - c} < \eta_1 < \frac{(c_s - V)\,(x_1 + ct)}{c_s + c} = \eta_R. \tag{3.10}$$

The position of x_1 within the interval $(-ct, c_s t)$ determines the extent to which the ellipsoid contributes to the integration; if $-ct < x_1 < ct$ then only part of the ellipsoid

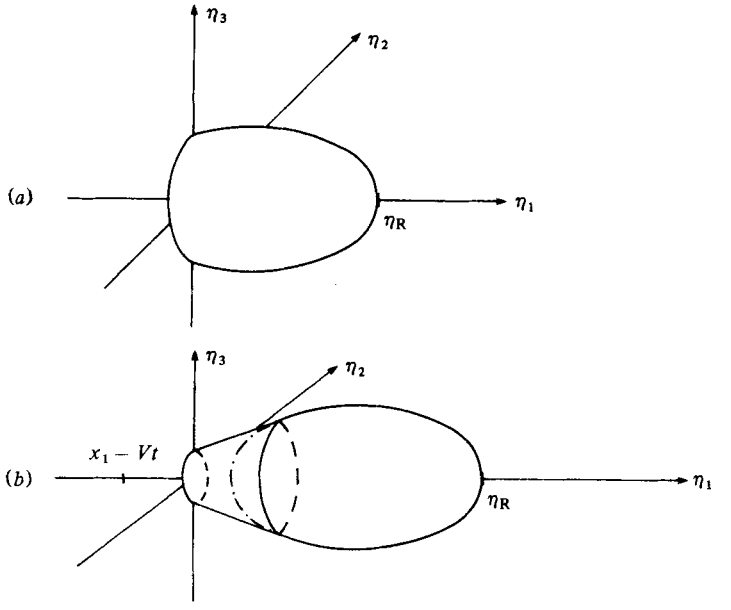

FIGURE 1. Quadrupole sources for piston flow. The regions of η-space from which quadrupoles radiate to the point $(\mathbf{x}, t)$. (*a*) Subsonic piston with $Vt < x_1 < ct$. (*b*) Supersonic piston with $x_1 < Vt$, the quadrupoles inside the ellipsoid radiate once only, the remainder within the frustum radiate twice.

is integrated over, but if $ct < x_1 < c_s t$ then the whole ellipsoid is involved. The cylindrical symmetry of (3.6) allows the η_1 and η_3 integrations to be written in the form

$$T_{ij}\int \frac{2\pi(1-M^2)\,R\,dR\,d\eta_1}{\{(\eta_1-x_1+Vt)^2+(1-M^2)\,R^2\}^{\frac{1}{2}}} = \frac{2\pi T_{ij}}{1-M^2}\int [\,|\{(\eta_1-x_1+Vt)^2+(1-M^2)\,R^2\}^{\frac{1}{2}}|\,]_{R=0}^{R_{\max}(\eta_1)}\,d\eta_1. \quad (3.11)$$

$R_{\max}(\eta_1)$ is obtained from (3.9) to give a final η_1 integration:

$$\frac{2\pi T_{ij}}{1-M^2}\int_{\eta_1>0}\left\{\left|\eta_1\frac{Vc_s-c^2}{c(c_s-V)}+\frac{c^2t-Vx_1}{c}\right|-|\eta_1-x_1+Vt|\right\}d\eta_1. \quad (3.12)$$

Note that the integrand changes its form as η_1 passes through $x_1 - Vt$. The values of the integral and its wave field are given in table 1.

Field position	Field integral, (3.6)	Field strength
$c_s t < x_1$	0	0
$ct < x_1 < c_s t$	$2\pi c^2 T_{11}\dfrac{(x_1-c_s t)^2}{c_s^2-c^2}$	$\Delta\rho$
$Vt < x_1 < ct$	$2\pi c^2 T_{11}\left\{t^2-\dfrac{(x_1+ct)^2}{2c(c_s+c)}-\dfrac{(x_1-ct)^2}{2c(c-V)}\right\}$	$\dfrac{\Delta\rho}{2c}\left\{-\dfrac{1}{c_s+c}-\dfrac{1}{c-V}\right\}$
$-ct < x_1 < Vt$	$2\pi c^2 T_{11}\left\{\dfrac{(x_1+ct)^2}{2c(c+V)}-\dfrac{(x_1+ct)^2}{2c(c_s+c)}\right\}$	$\dfrac{\Delta\rho}{2c}\left\{\dfrac{1}{c_s+c}+\dfrac{1}{c+V}\right\}$
$x_1 < -ct$	0	0

TABLE 1. Subsonic piston, quadrupole source

Field position	Field integral, (3.13)	Field strength
$ct < x_1 < c_s t$	$2\pi c^2 T_{11} \dfrac{(x_1 - c_s t)^2}{c_s^2 - c^2}$	$\Delta\rho$
$-ct < x_1 < ct$	$2\pi c^2 T_{11} \left\{ -\dfrac{(x_1+ct)^2}{2c(c_s+c)} + \dfrac{(x_1+ct)^2}{2c(c+c)} \right\}$	$\Delta\rho(c_s^2 - c^2) \left\{ -\dfrac{1}{2c(c_s+c)} + \dfrac{1}{4c^2} \right\}$

TABLE 2. Sonic piston, quadrupole source

A simplification is possible when the boundary moves sonically, i.e. $M = 1$. Then (3.6) reduces to

$$\int \left[\frac{T_{ij} H(f)}{r|1 - M_r|} \right]_{\text{ret}} d\eta^3 = \int \frac{[T_{ij} H(f)]}{|z \,.\, M|} d\eta^3 = \int \frac{[T_{ij}]\, 2\pi R \, dR \, d\eta_1}{|x_1 - ct - \eta_1|}, \tag{3.13}$$

and the η_1 integration becomes

$$\frac{\pi}{c_s - c} \int \operatorname{sgn}(\eta_1 - (x_1 - ct)) \{(c_s - c)(x_1 + ct) - (c_s + c)\eta_1\} d\eta_1. \tag{3.14}$$

The results table now has only two non-zero entries; see table 2.

When the boundary moves supersonically the basic integral takes the form

$$\int \left[\frac{T_{ij} H(f)}{r|1 - M_r|} \right]_{\text{ret}} d\eta^3 = \int \frac{[T_{ij}]\, d\eta^3}{\{(z \,.\, M)^2 - z^2(M^2 - 1)\}^{\frac{1}{2}}}. \tag{3.15}$$

The $\boldsymbol{\eta}$-frame now moves supersonically relative to the $\mathbf{y}$-frame. As a consequence the denominator of the integrand is real only for values of $\boldsymbol{\eta}$ that lie within the fore and aft Mach semi-cones of the point $\mathbf{x} - \mathbf{V}t$. The requirement that $\tau < t$ restricts the integration range to the aft semi-cone between $\mathbf{x} - \mathbf{V}t$ and the source. Both values of r given by (3.4) are now valid, signifying that each point of the $\boldsymbol{\eta}$-frame lying in this semi-cone can radiate to $\mathbf{x}$ twice. However, the unsteadiness of the stress source in the $\boldsymbol{\eta}$-frame limits these points to radiate to $\mathbf{x}$ either twice, once, or else not at all.

The region of $\boldsymbol{\eta}$-space that radiates once only to $(\mathbf{x}, t)$ is enclosed by the ellipsoid of revolution (3.9), again subject to $\eta_1 > 0$. The points that radiate twice to $(\mathbf{x}, t)$ occupy the region enclosed by the aft Mach semi-cone of $\mathbf{x} - \mathbf{V}t$ and the ellipsoid (3.9), also subject to $\eta_1 > 0$; see figure 1 (*b*). For these latter points the integral needs to be doubled to account for the repeated radiation. The final integration is

$$\frac{2\pi}{1 - M^2} \int [\{(x_1 - \eta_1 - Vt)^2 - (M^2 - 1) R^2\}^{\frac{1}{2}}]_{R=0}^{R(\eta_1)} d\eta_1, \tag{3.16}$$

where $R(\eta_1)$ traces out the radius appropriate for the cone or ellipsoid. Again the integrand changes its form as η_1 passes through $x_1 - Vt$. The non-zero results for the supersonic piston are given in table 3.

The significance of the four regions of field position given in table 3 is as follows:

$Vt < x_1 < c_s t$ no surface terms contribute, only quadrupoles radiate and these give the complete field;

$ct < x_1 < Vt$ surface terms radiate twice only;

$\dfrac{c^2 t}{V} < x_1 < ct$ surface terms may radiate once or twice;

$-ct < x_1 < \dfrac{c^2 t}{V}$ surface terms radiate once only.

Field position	Field integral (3.15)	Field strength
$Vt < x_1 < c_s t$	$2\pi c^2 T_{11} \dfrac{(x_1 - c_s t)^2}{c_s^2 - c^2}$	$\Delta\rho$
$ct < x_1 < Vt$	$-2\pi c^2 T_{11}(V^2 - c^2)\left\{\dfrac{(x_1 - c_s t)^2}{c_s^2 - c^2} - \dfrac{(x_1 - Vt)^2}{V^2 - c^2}\right\}$	$-\Delta\rho\left\{\dfrac{c_s^2 - c^2}{V^2 - c^2} - \dfrac{V^2 - c^2}{c_s^2 - c^2}\right\}$
$\dfrac{c^2 t}{V} < x_1 < ct$	$\pi c T_{11}(x_1 + ct)^2\left\{\dfrac{1}{V+c} - \dfrac{1}{c_s + c}\right\}$	$\Delta\rho \dfrac{(c_s^2 - c^2)}{2c}\left\{\dfrac{1}{V+c} - \dfrac{1}{c_s+c}\right\}$
$-ct < x_1 < \dfrac{c^2 t}{V}$	$\pi c T_{11}(x_1 + ct)^2\left\{\dfrac{1}{V+c} - \dfrac{1}{c_s + c}\right\}$	$\Delta\rho \dfrac{(c_s^2 - c^2)}{2c}\left\{\dfrac{1}{V+c} - \dfrac{1}{c_s+c}\right\}$

TABLE 3. Supersonic piston, quadrupole source

Field position	Monopole field strength	Dipole field strength
Subsonic piston		
$Vt < x_1 < ct$	$\dfrac{\Delta\rho(c_s - V)}{2(c - V)}$	$\dfrac{\Delta\rho c_s(c_s - V)}{2c(c - V)}$
$-ct < x_1 < Vt$	$\dfrac{\Delta\rho(c_s - V)}{2(c + V)}$	$-\dfrac{\Delta\rho c_s(c_s - V)}{2c(c + V)}$
Sonic piston		
$-ct < x_1 < ct$	$\dfrac{\Delta\rho(c_s - c)}{2c}$	$-\dfrac{\Delta\rho c_s(c_s - c)}{2c^2}$
Supersonic piston		
$ct < x_1 < Vt$	$\dfrac{\Delta\rho(c_s - V)\,V}{V^2 - c^2}$	$\dfrac{\Delta\rho c_s(c_s - V)}{V^2 - c^2}$
$\dfrac{c^2 t}{V} < x_1 < ct$	$\dfrac{\Delta\rho(c_s - V)}{2(V + c)}$	$-\dfrac{\Delta\rho(c_s - V)\,c_s}{2(V + c)\,c}$
$-ct < x_1 < \dfrac{c^2 t}{V}$	$\dfrac{\Delta\rho(c_s - V)}{2(V + c)}$	$\dfrac{\Delta\rho(c_s - V)\,c_s}{2(V + c)\,c}$

TABLE 4. Surface source

The evaluation of the surface integrals in (2.3) is now quite straightforward, since for these integrals the η_1 integration is restricted to the region $\eta_1 = 0$. For the subsonic piston, the monopole term is

$$\begin{aligned}\frac{\partial}{\partial t}\int\left[\frac{\rho_0 V}{r|1 - M_r|}\right]_{\text{ret}} d\eta^2 &= \frac{\partial}{\partial t}\int \frac{\Delta\rho(c_s - V)\,\delta(\eta_1)}{\{(\eta_1 - x_1 + Vt)^2 + (1 - M^2)\,((\eta_2 - x_2)^2 + (\eta_3 - x_3)^2)\}^{\frac{1}{2}}}\, d\eta^3 \\ &= \Delta\rho(c_s - V)\frac{\partial}{\partial t}\int \frac{2\pi R}{\{(x_1 - Vt)^2 + (1 - M^2)\,R^2\}^{\frac{1}{2}}}\, dR \\ &= \Delta\rho 2\pi \frac{c_s - V}{1 - M^2}\frac{\partial}{\partial t}\left\{\left|\frac{c^2 t - V x_1}{c}\right| - |x_1 - Vt|\right\}. \end{aligned} \tag{3.17}$$

Again the calculation of the field depends on the values of t and of x_1. The supersonic piston is treated similarly. The surface dipole of (2.3) can be evaluated as above with the replacement of $\partial/\partial t$ with $-\partial/\partial x_1$ and change of source strength to $\Delta\rho(c_s - V)\,c_s$. The results for the surface sources are summarized in table 4. The tabulated results

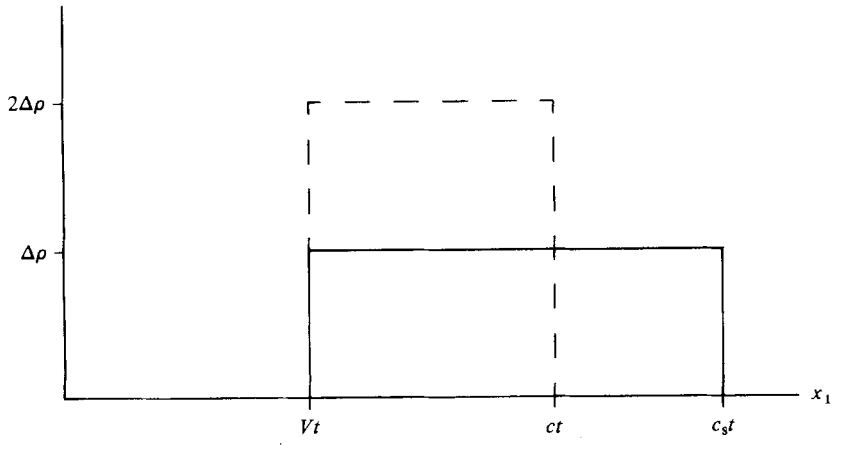

FIGURE 2. Schematic representation of the amplitudes and positions of the exact field and the surface induced field for the subsonic piston flow, $V = 0{\cdot}5\,c$. ——, exact field; – – –, surface-induced field.

indicate that fraction of the field appearing to originate in the various source terms. Figure 2 displays the combined dipole and monopole fields in the region of acoustic influence in front of a subsonic piston. The quadrupole field for this case is always negative, restoring the field generated at the surface to unity, and becomes increasing necessary for higher piston speeds. These values can be changed significantly and simplified by adopting a slightly modified analogy.

4. Modified analogy for one-dimensional flow

The derivation of (2.1) requires the introduction of a parameter c as the phase speed of the wave operator. The same parameter must necessarily occur in the definition of the quadrupole strength T_{ij} where it multiplies an isotropic component. The usual value chosen for the phase speed c is the ambient sound speed of the fluid. This choice makes a physical interpretation of the analogy plausible, for it causes the analogous sources to vanish in those regions of the flow where the disturbances are purely acoustic, and also causes the acoustic waves of the analogy, as governed by the wave operator, to travel at the speed of those being modelled.

However, an arbitrary choice of phase speed is equally correct although less intuitive. In fact the speed may even be negative; see Ffowcs Williams (1976). In these cases the quadrupole distribution is generally significant in all perturbed regions and plays an important role by producing a wave field that appears to travel at a speed different from that of its constituent wavelets.

The choice of phase speed affects the analogy in two ways: through its occurrence in the wave operator and the associated Green function it influences the field by controlling the interval over which a particular source element radiates, and through its appearance in the strength of the quadrupole it controls the analogous volume sources. The one-dimensional model flow serves to illustrate the effects of choosing a different phase speed. Putting $c = c_s$, (2.1) becomes

$$\left(\frac{\partial^2}{\partial\tau^2} - c_s^2\frac{\partial^2}{\partial y^2}\right)\{(\rho-\rho_0)\,H\} = -\frac{\partial}{\partial y_i}\left\{p_{ij}\frac{\partial H}{\partial y_i}\right\} + \frac{\partial}{\partial\tau}\left\{\rho_0 v_i\frac{\partial H}{\partial y_i}\right\}. \tag{4.1}$$

The only sources in this analogy are at the moving boundary, and there are no mechanisms of sound generation in the uniform flow behind the shock, so it is, in this case, rather misleading to regard the quadrupole source as representing elements that create waves. It is only the 'wrong' choice of phase speed for the problem that creates the non-zero stress and the resulting quadrupole-driven field. The shock wave travels with speed c_s, and this is the phase speed of the physical problem. When it is adopted in the analogy, the stress field vanishes and all the sources are satisfactorily confined to the boundary.

Increasing the phase speed of the wave operator causes the compactness of the sources to increase, and since $V < c_s$ the piston cannot now move supersonically. In front of the piston, $Vt < x_1 < c_s t$, the monopole and dipole of the modified analogy in (4.1) contribute identical terms of $\frac{1}{2}\Delta\rho$ each, while behind the piston, $c_s t < x_1 < Vt$, they contribute equal and opposite values of magnitude

$$\frac{\Delta\rho(c_s - V)}{2(c_s + V)}.$$

In a recent paper Ffowcs Williams (1979) discusses a different approach to the acoustic analogy in which only quadrupole sources are used. The surface sources are replaced by quadrupoles within the body. The interior quadrupoles are generally stronger than the exterior quadrupoles of the fluid flow, but the exterior quadrupoles can occupy a greater volume than the interior ones.

The conclusion is drawn that, except for flows where the exterior quadrupole-strength density is comparable to the interior strength density, any extensive region of weak quadrupoles is primarily a phase-shifting device. It is certainly true that in the flow model examined here the only role of the quadrupoles is that of a phase shift, and by recognizing the complete equivalence of (2.1) and (4.1) the view of the problem that was given tentatively by Ffowcs Williams is confirmed.

5. Two-dimensional flow

The second flow field considered is two-dimensional and steady. Inviscid compressible fluid, at rest, with density ρ_1 and pressure p_1, is disturbed by an infinite wedge, of angle α, which moves parallel to its lower surface into the fluid with a supersonic speed V. The wedge moves sufficiently fast for a plane shock to exist attached to the apex of the wedge, making an angle β with the direction of motion. When viewed from a frame moving with the wedge the flow is steady with the shock deflecting the incident flow through an angle α and compressing it to density ρ_2 and pressure p_2; see figure 3.

To determine the analogous sources, the atmospheric frame in which the undisturbed fluid is at rest is used. In this frame the shock has a normal velocity $c_s = V\sin\alpha$, and the disturbed fluid between the shock and the upper wedge surface has a velocity $U = V\sin\alpha/\cos(\beta-\alpha)$ normal to the shock. The sources are again most conveniently expressed in terms of $\Delta\rho$ and V. Mass and momentum conservation at the shock furnish

$$\rho_2 U = \Delta\rho c_s, \tag{5.1a}$$

$$\Delta p = p_2 - p_1 = \rho_1 c_s U, \tag{5.1b}$$

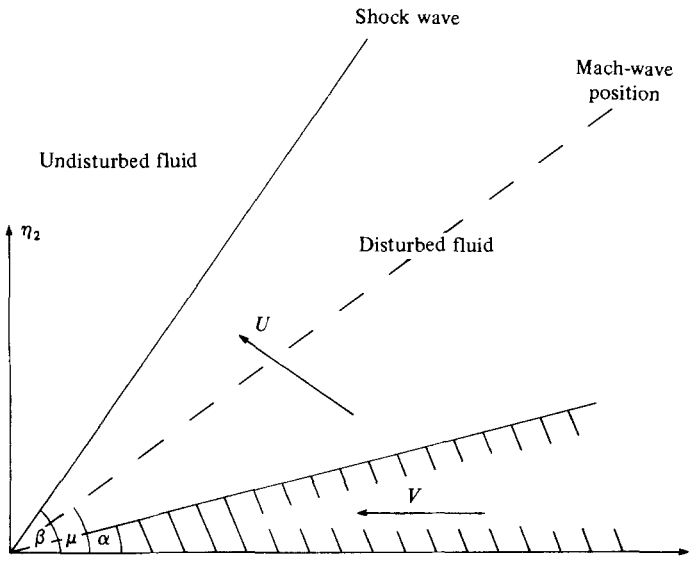

FIGURE 3. Geometry of wedge flow. A wedge of angle α moves supersonically at speed V, associated Mach angle μ. A plane shock is attached to the wedge apex and makes an angle β with the base of the wedge. The undisturbed fluid is compressed and accelerated to velocity **U** on crossing the shock.

giving

$$\rho_2 U^2 = \Delta\rho \frac{V^2 \sin\alpha \sin\beta}{\cos(\beta-\alpha)}, \tag{5.2a}$$

$$\Delta p = \Delta\rho \frac{V^2 \cos\beta \sin\beta \sin(\beta-\alpha)}{\cos(\beta-\alpha)}, \tag{5.2b}$$

$$\rho_1 = \Delta\rho \frac{\cos\beta \sin(\beta-\alpha)}{\sin\alpha}. \tag{5.2c}$$

With the 1-axis direction taken parallel to the flow of the disturbed fluid, the non-zero components of the Lighthill stress T_{ij} are

$$T_{11} = \Delta\rho\{V^2 \sin^2\beta - c^2\} = \Delta\rho(c_s^2 - c^2), \tag{5.3a}$$

$$T_{22} = T_{33} = \Delta p - c^2 \Delta\rho\delta_{i1} = \Delta\rho\{c_s(c_s - U) - c^2\delta_{ij}\}. \tag{5.3b}$$

Since the fluid flow, and therefore the analogous sources, become steady in a frame moving with the wedge, it is easier to evaluate the field at a point $\boldsymbol{\xi}$ fixed in the wedge frame, i.e. moving with the wedge when viewed from the **y**-frame. Using the transformations for the field derivatives

$$\left.\frac{\partial}{\partial x_i}\right|_t = \left.\frac{\partial}{\partial \xi_i}\right|_t, \quad \left.\frac{\partial}{\partial t}\right|_\xi = \left.\frac{\partial}{\partial t}\right|_x + V_i \left.\frac{\partial}{\partial x_i}\right|_x = 0. \tag{5.4}$$

expression (2.2) becomes

$$4\pi c^2 H(f)\tilde{\rho}(\boldsymbol{\xi}) = \frac{\partial^2}{\partial\xi_i \partial\xi_j}\int \frac{T_{ij}}{r} H(f)\delta(g)\,d\eta^3 d\tau$$
$$- \frac{\partial}{\partial\xi_i}\int \frac{p_{ij}}{r}\frac{\partial f}{\partial\eta_j}\delta(f)\delta(g)\,d\eta^3 d\tau - V_i \frac{\partial}{\partial\xi_i}\int \frac{\rho_0 v_i}{r}\frac{\partial f}{\partial\eta_i}\delta(f)\delta(g)\,d\eta^3 d\tau. \tag{5.5}$$

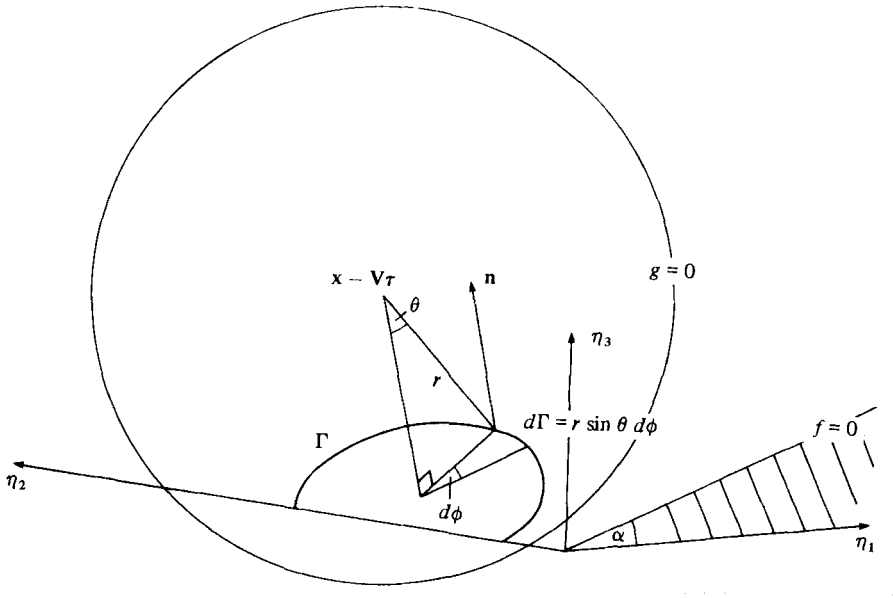

FIGURE 4. Geometry of the curve Γ. In η-space, at time τ, the sphere $g = 0 (r = c(t-\tau))$, centre $\mathbf{x}-\mathbf{V}\tau$, intersects the half-plane $f = 0 (-\eta_1 \sin\alpha + \eta_2 \cos\alpha = 0, \eta_1 > 0)$ along the circular arc Γ. Sources on Γ radiate to $\mathbf{x}-\mathbf{V}\tau$ along directions making an angle θ with the normal **n**.

The integrals can be projected onto the appropriate (Ω, τ)- and (Γ, τ)-subspaces according to (2.4), giving

$$4\pi c^2 H(f)\tilde{\rho}(\boldsymbol{\xi}) = \frac{\partial^2}{\partial\xi_i \partial\xi_j}\int \frac{T_{ij}}{r} c\, d\Omega d\tau - \frac{\partial}{\partial\xi_i}\int \frac{p_{ij}}{r}\frac{\partial f}{\partial\eta_j}\frac{c\, d\Gamma\, d\tau}{\sin\theta} + V_j \frac{\partial}{\partial\xi_j}\int \frac{\rho_0 v_i}{r}\frac{\partial f}{\partial\eta_i}\frac{c\, d\Gamma\, d\tau}{\sin\theta}. \quad (5.6)$$

The surface integrals are evaluated first. They combine to give

$$\left\{\Delta p\left(\sin\alpha\frac{\partial}{\partial\xi_1} - \cos\alpha\frac{\partial}{\partial\xi_2}\right) + \rho_1 V^2 \sin\alpha\frac{\partial}{\partial\xi_1}\right\}\int \frac{c\, d\Gamma\, d\tau}{r\sin\theta}, \quad (5.7)$$

where the directions of ξ_1 and η_1 are parallel to the incident flow as observed in the wedge frame, so that $\partial f/\partial\eta_i = (-\sin\alpha, \cos\alpha, 0)$ and $\mathbf{V} = (-V, 0, 0)$.

Now $(r\sin\theta)^{-1} d\Gamma$ is the angular element $d\phi$ subtended by the arc element $d\Gamma$ on the upper surface of the wedge; see figure 4. Hence $\int (r\sin\theta)^{-1} d\Gamma\, d\tau$ can be rewritten as $\int d\phi\, d\tau = \int \Delta\tau(\phi)\, d\phi$, where $\Delta\tau(\phi)$ is the time interval for which that surface element whose azimuthal position is ϕ radiates to $\boldsymbol{\xi}$. After much algebra (5.7) evaluates to

$$\left\{\Delta p\left(\sin\alpha\frac{\partial}{\partial\xi_1} - \cos\alpha\frac{\partial}{\partial\xi_2}\right) + \rho_1 V^2 \sin\alpha\frac{\partial}{\partial\xi_1}\right\}\frac{2\pi\tan\mu}{\sin(\mu-\alpha)}\{\xi_1\sin\mu - \xi_2\cos\mu\}, \quad (5.8)$$

where μ is the Mach angle corresponding to the speed of the wedge. Hence the surface sources cause a density disturbance

$$\frac{\tan\mu}{2c^2\sin(\mu-\alpha)}\{\Delta p\cos(\mu-\alpha) + \rho_1 V^2 \sin\alpha\sin\mu\}. \quad (5.9)$$

This field is confined to a region within the Mach wave of the wedge apex, since it is a disturbance propagating at the ambient speed of sound.

The volume distribution of quadrupoles generates the whole density perturbation when ξ lies behind the shock wave and ahead of the Mach wave; but when ξ lies within the Mach-wave region above the wedge, that quadrupole contribution is

$$-\tan\mu\left\{\frac{\cos(\beta+\mu)}{\sin(\beta+\mu)}[\rho_2 U^2+\Delta p-c^2\Delta\rho]+\frac{1}{\sin(\mu-\alpha)}\right.$$
$$\left.\times[\rho_2 U^2\cos(\beta-\alpha)\cos(\beta-\mu)+(\Delta p-c^2\Delta\rho)\cos(\mu-\alpha)]\right\}. \quad (5.10)$$

Within the wedge, and below its lower surface the fields of the analogous sources cancel to give zero perturbation.

6. Alternative source descriptions

In the absence of an underlying physical basis to the source description of (2.1) it is conceivable that it may not be the most useful description when boundaries are present in the flow. In fact the sources of (2.1) may be reformulated in a variety of ways. For instance, in their original paper, Ffowcs Williams & Hawkings, examining the Mach wave generated by a rigid impermeable surface, expressed the monopole source as volume dipole and quadrupole sources within the body. This is possible because the monopole has zero total instantaneous strength; but for the general case any advantages of this description are uncertain.

Two alternative systems of analogous sources that de-emphasize the explicit quadrupole component of (2.1) are now examined using the wedge-flow problem. The first alternative system rewrites the volume quadrupole source of (2.1) as a volume dipole source together with a surface dipole at the boundary of the fluid:

$$\frac{\partial^2}{\partial y_i\partial y_j}\{T_{ij}H(f)\}=-\frac{\partial}{\partial y_i}\left\{-\frac{\partial T_{ij}}{\partial y_j}H(f)\right\}-\frac{\partial}{\partial y_i}\left\{-T_{ij}\frac{\partial f}{\partial y_j}\delta(f)\right\}. \quad (6.1)$$

The analogous sources of (2.1) then become

$$-\frac{\partial}{\partial y_i}\left\{-\frac{\partial T_{ij}}{\partial y_j}H(f)\right\}-\frac{\partial}{\partial y_i}\left\{(-\rho u_i u_j+c^2\delta_{ij}\Delta\rho)\frac{\partial f}{\partial y_j}\delta(f)\right\}+\frac{\partial}{\partial\tau}\left\{\rho_0 v_i\frac{\partial f}{\partial y_i}\delta(f)\right\}. \quad (6.2)$$

The surface-located sources now involve the fluid velocity and density at the bounding surface, but not the surface pressure.

Applying this system to the wedge flow, in the region between the Mach line of the apex and the upper surface of the wedge this new surface dipole contributes to the field a component

$$\frac{-1}{4\pi c^2}\frac{\partial}{\partial\xi_i}\int(-\rho_2 u_i u_j+c^2\Delta\rho\delta_{ij})\frac{\partial f}{\partial\eta_j}\frac{c\,d\Gamma\,d\tau}{r\sin\theta}$$
$$=\left\{\frac{\rho_2 V^2\sin^2\alpha}{\cos(\beta-\alpha)}\left(-\sin\beta\frac{\partial}{\partial\xi_1}+\cos\beta\frac{\partial}{\partial\xi_2}\right)+\Delta\rho c^2\left(-\sin\alpha\frac{\partial}{\partial\xi_1}+\cos\alpha\frac{\partial}{\partial\xi_2}\right)\right\}$$
$$\times\frac{\tan\mu}{2\pi c^2\sin(\mu-\alpha)}\{\xi_1\sin\mu-\xi_2\cos\mu\}$$
$$=\tfrac{1}{2}\Delta\rho\left\{-\frac{\sin\alpha\sin\beta\cos(\beta-\mu)}{\sin\mu\cos\mu\sin(\mu-\alpha)}+\frac{\sin 2\beta\tan(\beta-\alpha)}{\sin 2\mu\tan(\mu-\alpha)}\right\}. \quad (6.3)$$

The uniform stress field makes the volume dipole strength $\partial T_{ij}/\partial y_j$ non-zero only at the shock front, so the integration for the volume dipoles takes the form $\int \ldots d\Gamma\, d\tau$, where Γ is the intersection of the shock and the sonic surface $r = c(t-\tau)$. This component of the source generates the complete radiated field in the region between the shock and the apex Mach line, and a component

$$\tfrac{1}{2}\Delta\rho\left(1-\frac{\sin 2\beta}{\sin 2\mu}\right) \tag{6.4}$$

between the apex Mach line and the upper wedge surface.

This interpretation of the analogous sources demonstrates the point made by Ffowcs Williams & Hawkings when referring to the estimation of the wave field generated by a high-speed surface; the field derivatives acting on the quadrupole integral produce further integrals at the surface of the body. Here the sources have been manipulated to isolate the additional dipole surface terms but this has required the replacement of the volume quadrupoles with volume dipoles.

A second alternative system ignores the multipole classification of the source terms and evaluates their fields directly as if they were just simple sources. The two surface terms of (2.1), when expressed in the $\boldsymbol{\eta}$-co-ordinate frame in which the wedge is at rest, have forms similar to each other that combine as

$$-\frac{\partial}{\partial\eta_i}\left(\Delta p\delta_{ij}\frac{\partial H}{\partial\eta_j}\right)-v_j\frac{\partial}{\partial\eta_j}\left(\rho_1 v_i\frac{\partial H}{\partial\eta_i}\right)=-\{\Delta p\delta_{ij}+\rho_1 v_i v_i\}\frac{\partial}{\partial\eta_i}\frac{\partial}{\partial\eta_j}H(f). \tag{6.5}$$

Equations (2.3) and (3.15) may be used to obtain the field as

$$\frac{1}{2\pi c^2}\int -\frac{\{\Delta p\delta_{ij}+\rho_1 v_i v_j\}}{\{z_1^2-(M^2-1)(z_2^2+z_3^2)\}^{\frac{1}{2}}}\frac{\partial^2 H(f)}{\partial\eta_i\partial\eta_j}\,dz^3. \tag{6.6}$$

The range of integration is over those $\mathbf{z}$ for which the denominator is real, as in the one-dimensional problem. This region is the aft Mach cone of the point $\boldsymbol{\xi}$. Integrating out the z_3 dependence gives

$$-\frac{\{\Delta p\delta_{ij}+\rho_1 v_i v_j\}}{2c^2(M^2-1)^{\frac{1}{2}}}\int\frac{\partial^2 H(f)}{\partial z_i\partial z_j}\,dz_1 dz_2, \tag{6.7}$$

where $g > 0$ lies in the (z_1, z_2)-plane bounded by the lines

$$g_\pm = (\eta_1-\xi_1)\sin\theta \mp (\eta_2-\xi_2)\cos\theta.$$

Integration by parts then gives

$$\frac{\{\Delta p\delta_{ij}+\rho_1 v_i v_j\}}{2c^2(M^2-1)^{\frac{1}{2}}}\int\frac{\partial H(f)}{\partial z_i}\frac{\partial H(g)}{\partial z_j}\,dz_1 dz_2=\frac{\{\Delta p\delta_{ij}+\rho_1 v_i v_j\}}{2c^2(M^2-1)^{\frac{1}{2}}}\int\frac{\partial f}{\partial z_i}\frac{\partial g}{\partial z_j}\,\delta(f)\,\delta(g)\,dz_1 dz_2. \tag{6.8}$$

There are two cases to consider; either $\boldsymbol{\xi}$ lies above the wedge, or $\boldsymbol{\xi}$ lies below the wedge, in which cases $g = g_+$ or $g = g_-$ respectively should be used. Changing the co-ordinates to f and $g_\pm$ requires use of the relation

$$dz_1 dz_2 = \frac{df\,dg_\pm}{|\sin(\mu\pm\alpha)|}, \tag{6.9}$$

and gives the field at $(\boldsymbol{\xi}, t)$ as

$$\frac{\tan\mu}{2c^2|\sin(\mu\mp\alpha)|}\{\pm\Delta p\cos\alpha+\rho_1 V^2\sin\alpha\sin\mu\}. \tag{6.10}$$

The component of (6.10) attributable to the dipole term of (2.1) is

$$\pm \frac{\Delta\rho \sin 2\beta \tan(\beta-\alpha)\cos(\mu-\alpha)}{2\sin 2\mu|\sin(\mu\mp\alpha)|}, \tag{6.11}$$

and that attributable to the monopole term is

$$\frac{\Delta\rho\cos\beta\sin(\beta-\alpha)}{2\cos\mu|\sin(\mu\mp\alpha)|}. \tag{6.12}$$

The remaining source $\partial^2\{T_{ij}H(f)\}/\partial y_i\partial y_j$ has non-zero components at the shock and upper wedge surface. The shock gives an effective source, when viewed in the wedge frame, of

$$T_{ij}\frac{\partial^2 H(s)}{\partial\eta_i\partial\eta_j}, \quad s=-\eta_1\sin\beta+\eta_2\cos\beta, \tag{6.13}$$

which gives a field, using the above method, of

$$\frac{T_{ij}\tan\mu}{2c}\int\frac{\partial s}{\partial z_j}\frac{\partial g_\pm}{\partial z_i}\delta(s)\,\delta(g_\pm)\frac{ds\,dg_\pm}{|\sin(\beta\mp\mu)|}.$$

In the region of Mach-wave influence, only the g_+ component counts, and the field is

$$-\frac{\Delta\rho(c_s^2-c^2)\tan\mu\cos(\beta+\mu)}{2c^2|\sin(\beta+\mu)|}. \tag{6.14}$$

Similarly, the effective source at the upper wedge surface is $T_{ij}\partial^2 H(f)/\partial\eta_i\partial\eta_j$, which generates a field

$$\frac{\Delta\rho\tan\mu}{2c^2|\sin(\mu+\alpha)|}\{\rho_2U^2\cos(\beta-\alpha)\cos(\beta+\mu)+(\Delta p-c^2\Delta\rho)\cos(\mu+\alpha)\} \tag{6.15a}$$

below the wedge surface, and

$$-\frac{\Delta\rho\tan\mu}{2c^2|\sin(\mu-\alpha)|}\{\rho_2U^2\cos(\beta-\alpha)\cos(\beta-\mu)+(\Delta p-c^2\Delta\rho)\cos(\mu-\alpha)\} \tag{6.15b}$$

between the apex Mach line and the upper wedge surface.

Only the shock-located source is able to radiate to the region between the shock and the apex Mach line, and it does so in a manner identical to the one-dimensional shock to generate the complete field. All four components of the source can radiate to the region between the apex Mach line and the upper wedge surface, and their overall perturbation is $\Delta\rho$. In the Mach-wave region within and below the wedge the total radiated field is zero, as it should be.

7. Fields of wedge-flow sources

Three source systems have been introduced:

(1) volume quadrupoles, surface dipoles, and surface monopoles, as in (2.1);

(2) volume dipoles, surface dipoles, and surface monopoles, as in (6.2);

(3) simple sources, as in (6.5) and (6.13).

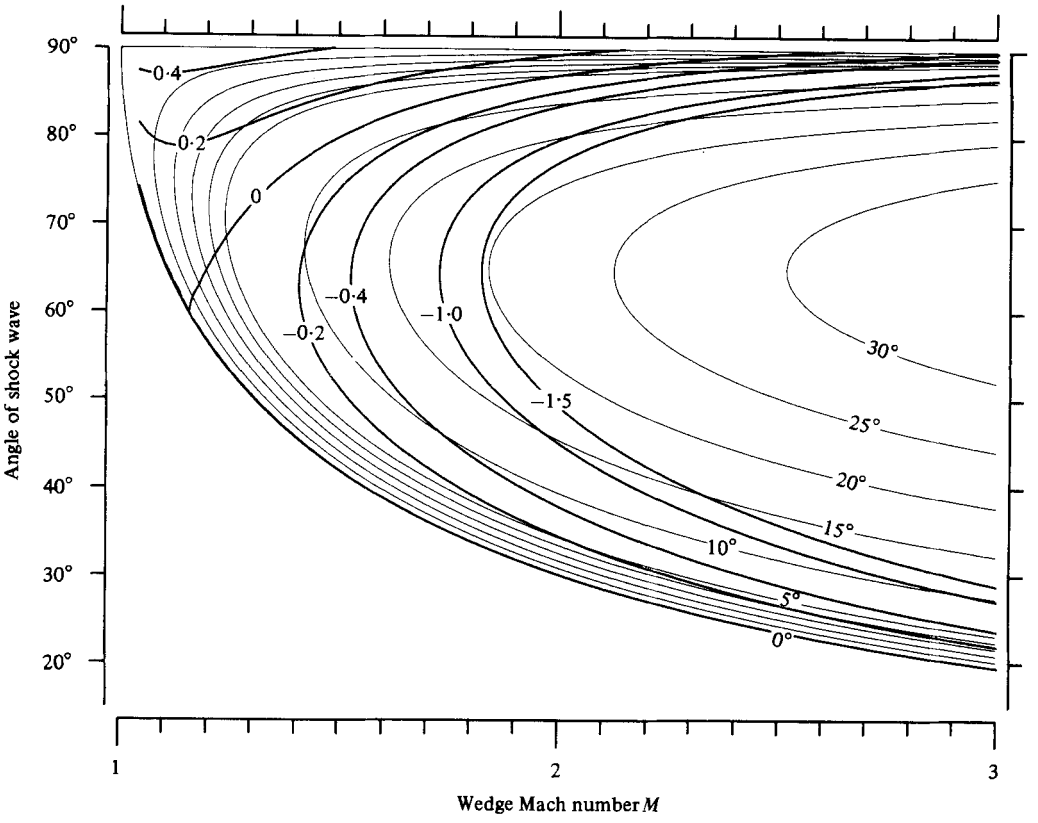

FIGURE 5. The wave amplitude, within the Mach-wave region, due to the total-quadrupole source, expressed as a fraction of the real amplitude $\Delta\rho$, (thick contours); and the shock-wave angle β, plotted for constant wedge angle α, (thin contours) as a function of the Mach number M.

The discussion of the two model problems shows that only for system (3) can the fields of all the source terms be obtained easily. The fields arising from the sources of (1) and (2) can be determined by suitable combinations of the fields of (3). The sources of (3) for the models are as follows.

(i) A source located at the shock and a similar source at the wedge upper surface. Together these are equivalent to the volume quadrupoles of (1), and also to the volume dipoles, and part of the surface dipoles of (2).

(ii) A surface dipole common to (1), (2) and (3).

(iii) A surface monopole, also common to all three systems. For the wedge flow, in the region between the apex Mach line and the upper wedge surface, the magnitudes of the fields of the four sources of (3) are:
for the shock-located source

$$\tfrac{1}{2}\Delta\rho\left(1-\frac{\sin 2\beta}{\sin 2\mu}\right); \tag{7.1a}$$

for the quadrupole discontinuity at the wedge surface

$$\tfrac{1}{2}\Delta\rho\left(\frac{\tan\mu}{\tan(\mu-\alpha)}-\frac{\sin\alpha\sin\beta\cos(\beta-\mu)}{\sin\mu\cos\mu\sin(\mu-\alpha)}-\frac{\sin 2\beta\tan(\beta-\mu)}{\sin 2\mu\tan(\mu-\alpha)}\right); \tag{7.1b}$$

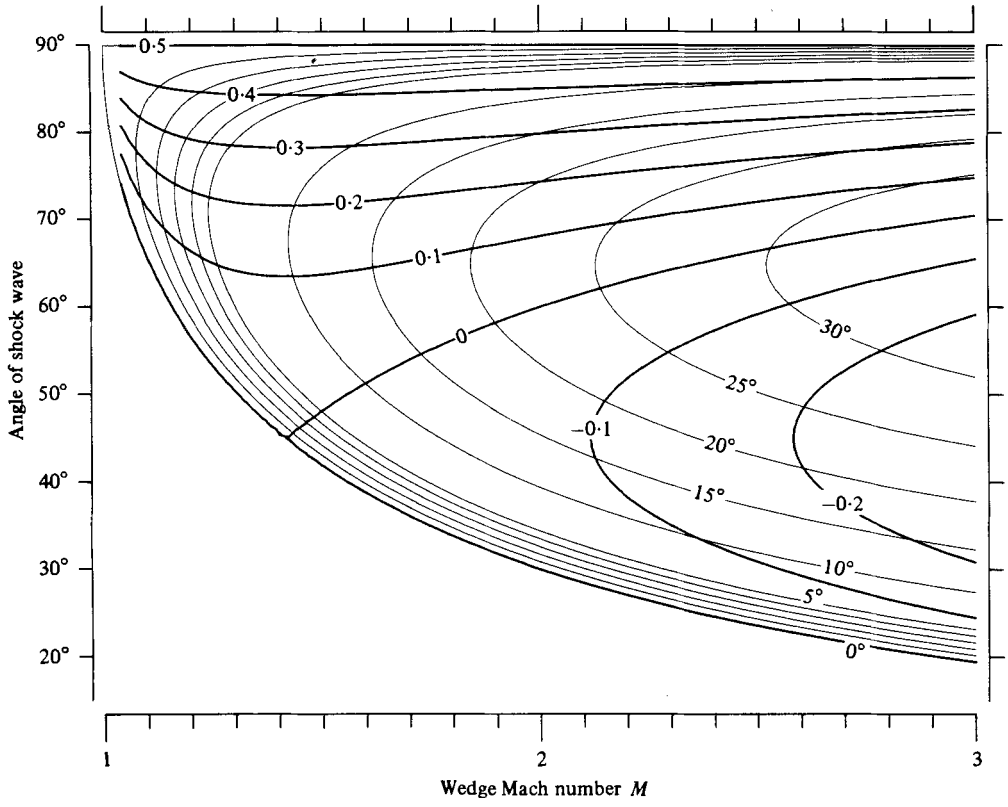

FIGURE 6. The wave amplitude, within the Mach-wave region, due to the shock-quadrupole source, expressed as a fraction of the real amplitude $\Delta\rho$, (thick contours); and the shock wave angle β, plotted for constant wedge angle α, (thin contours) as a function of the Mach number M.

for the original surface dipole

$$\tfrac{1}{2}\Delta\rho\,\frac{\sin 2\beta\tan(\beta-\alpha)}{\sin 2\mu\tan(\mu-\alpha)}; \tag{7.1c}$$

and for the original surface monopole

$$\tfrac{1}{2}\Delta\rho\left(\frac{\cos\beta\sin(\beta-\alpha)}{\cos\mu\sin(\mu-\alpha)}\right). \tag{7.1d}$$

The independent parameters are the wedge angle α, and the wedge speed cM, or equivalently the Mach angle $\mu = \arcsin(M^{-1})$. The four fields of (7.1) are plotted in figures 6–8 and 10. The quadrupole, dipole, and monopole fields of (2.1) are plotted in figures 5, 8 and 10. They show that for thin wedges, $\alpha < 5°$, and upper transonic speeds, $1{\cdot}0 < M < 1{\cdot}5$, the quadrupole sources contribute at most 20 %, either positively or negatively, of the actual wave amplitude. The corresponding dipoles generate over half of the wave, and the monopole component increases through half as the wedge speed increases. For very thin wedges the monopole and dipole dominate the final field.

In systems (2) and (3) the conventional quadrupole source is divided into shock and surface located sources. For system (2) the shock constitutes the volume dipole source,

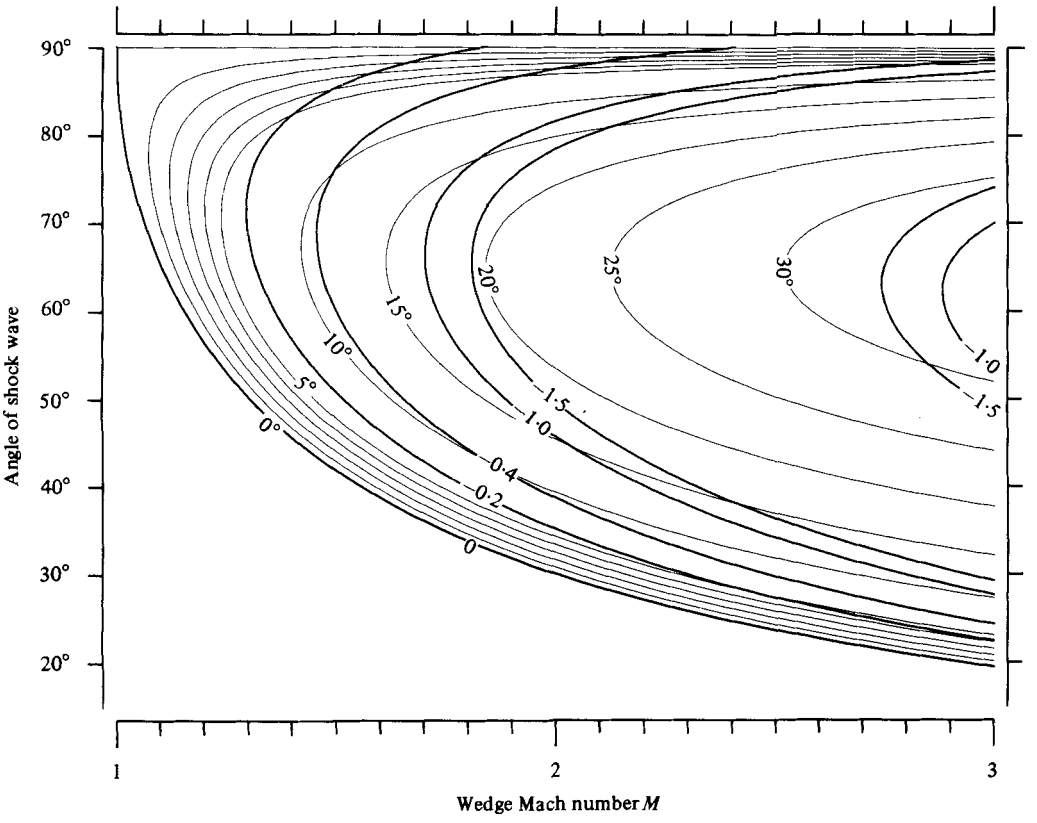

FIGURE 7. The wave amplitude, within the Mach-wave region, due to the surface-quadrupole source, expressed as a fraction of the real amplitude $\Delta\rho$, (thick contours); and the shock-wave angle β, plotted for constant wedge angle α, (thin contours) as a function of the Mach number M.

and the remainder of the quadrupole component is concentrated at the wedge surface. Their fields are plotted in figures 6 and 7. In the above flow regime these fields are relatively weak, amounting to between $-10\,\%$ and $+20\,\%$ of the final amplitude for the shock and $-20\,\%$ to $0\,\%$ for the surface quadrupole, which is always negative.

A comparison is made between the surface dipole field described in (2.1) using the exact flow details and the equivalent dipole field derived from a linear estimate of the surface pressure

$$p_{\text{lin}} = \frac{\rho_1 V^2 \alpha}{(M^2-1)^{\frac{1}{2}}}. \tag{7.2}$$

The linearized field is almost half the size of its exact counterpart for thin wedges at low supersonic speeds, see figure 9.

For a constant wedge speed, as the wedge angle increases the exact surface dipole and surface quadrupole fields both increase in magnitude but their opposite signs cause them to interfere destructively. This suggests, perhaps, that system (2) may be more useful than systems (1) and (3).

The various fields are also calculated and plotted in figures 5–10 for the cases of the wedge supporting a strong shock. Here the quadrupoles are more dominant than those of the weak flows, especially for thin wedges in the speed range $1{\cdot}0 < M < 2{\cdot}0$,

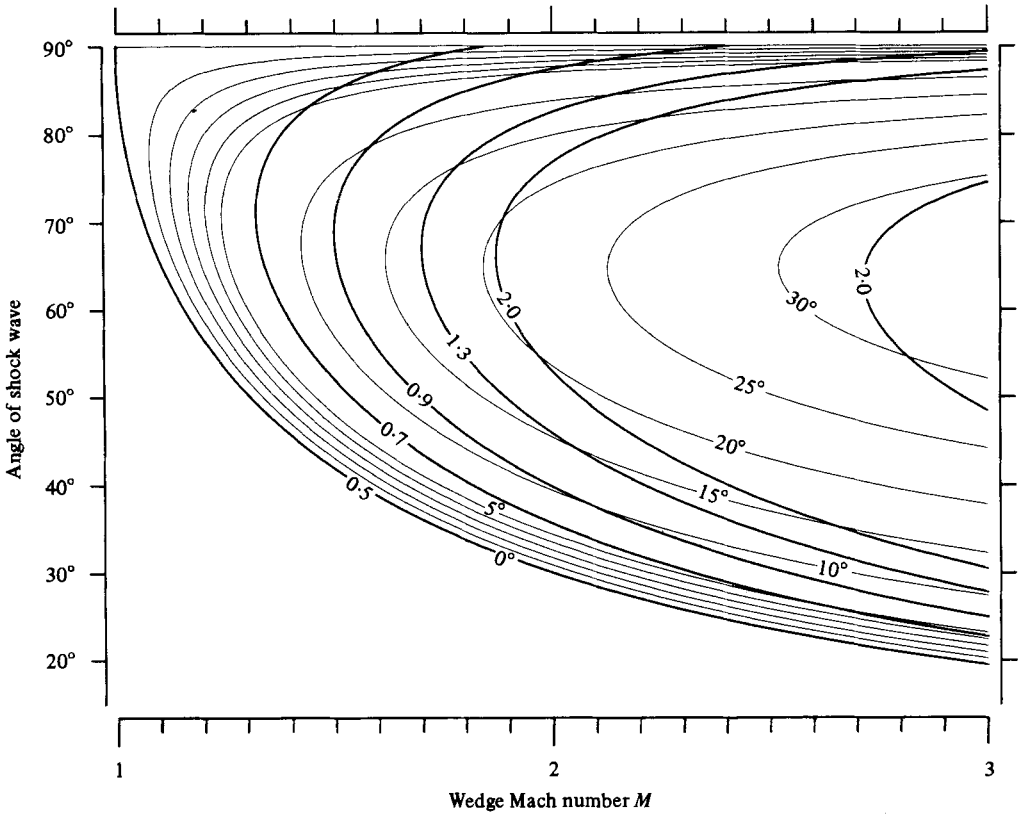

FIGURE 8. The wave amplitude, within the Mach-wave region, due to the exact-surface-dipole source, expressed as a fraction of the real amplitude $\Delta\rho$, (thick contours); and the shock-wave angle β, plotted for constant wedge angle α, (thin contours) as a function of the Mach number M.

where the quadrupole component of the wave can approach half the total wave amplitude. For these cases the dipole is the dominant term, giving typically 70 % of the wave, and the monopoles at most 20 %.

8. Phase shifts induced by quadrupoles

The model flows discussed are created in practice by moving boundaries, yet the source systems discussed require sources to exist within the fluid as well as at the bounding surfaces. These volume sources are due to non-linear features of the flow, and are the quadrupoles of (2.1). In the piston problem, choosing the phase speed of the analogy to match the shock speed of the disturbed fluid eliminates the quadrupole source distribution and confines the sources to the boundary.

That the volume quadrupoles are related to the phase speed of a propagating wave is a feature that first arose in Lighthill's (1953) treatment of sound scattering by turbulence. His model, in which the wavelets propagate with a constant phase speed, led to the following dilemma; when the phase speeds of the incident sound pulse and the scattered wave were identical a singularity arose in the forward scattered wave. For the case of a shock propagating through turbulence Lighthill argued that the difference between the speed of a shock and that of the acoustic wavelets would avoid the singu-

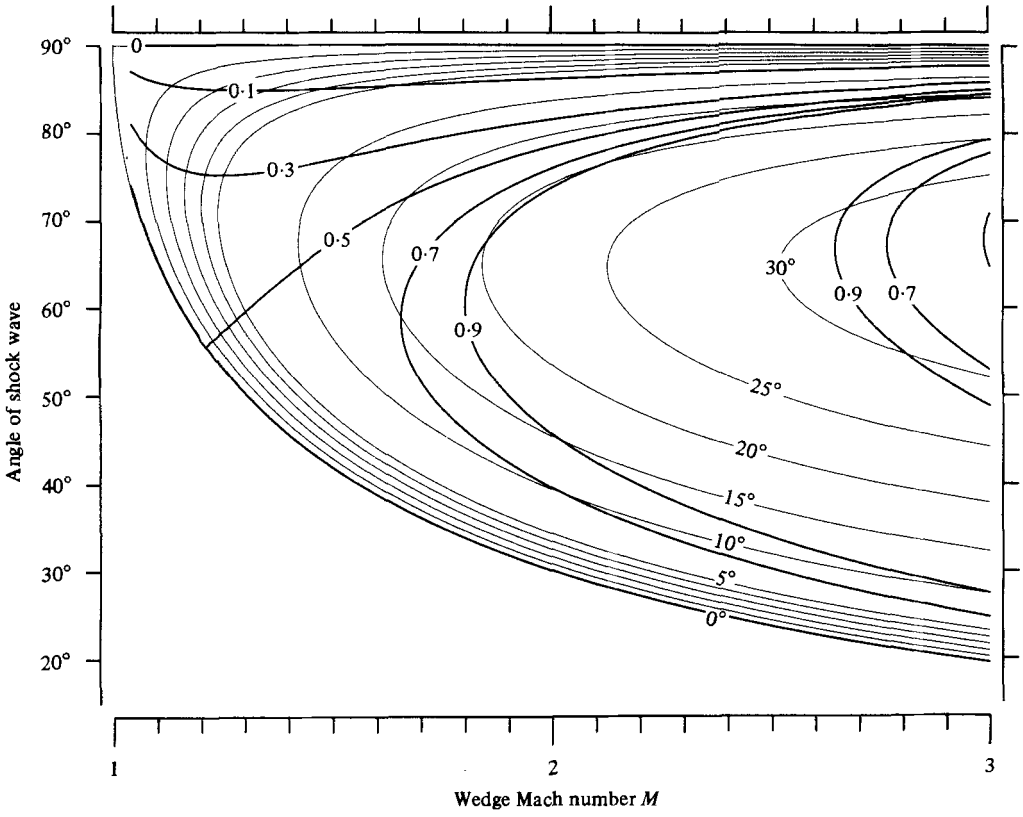

FIGURE 9. The wave amplitude, within the Mach-wave region, due to the linearized-surface-dipole source, expressed as a fraction of the real amplitude $\Delta\rho$, (thick contours); and the shock-wave angle β, plotted for constant wedge angle α, (thin contours) as a function of the Mach number M.

larity, but he gave no prescription for the general resolution of the difficulty. Crow (1969) tackled a similar problem with the same quadrupole scattering mechanism, and revealed the singularity to be integrable. The integrated value gave, to first order in the scattering variable, the displacement of the incident wave due to turbulent convection and local variations in the speed of sound. Crow thereby demonstrated that an acoustic disturbance propagating across a turbulent region is displaced because of phase-speed variations in the turbulence as well as being scattered, the phase-speed variations occurring at the same order of approximation as the scattering. An incident step wave $H(x+ct)$ is displaced by the turbulence in which it moves with phase speed c_t to

$$H\left(x+ct+\int^t (c_t-c)\,d\tau\right). \tag{8.1}$$

When this is expanded in a perturbation series as

$$H(x+ct)+(c_t-c)\,dt\,\delta(x+ct)+\ldots \tag{8.2}$$

the singular first-order scattering term can be seen in its true perspective. The scattering appears to produce a pulse-like wave that is in fact only part of a series expansion

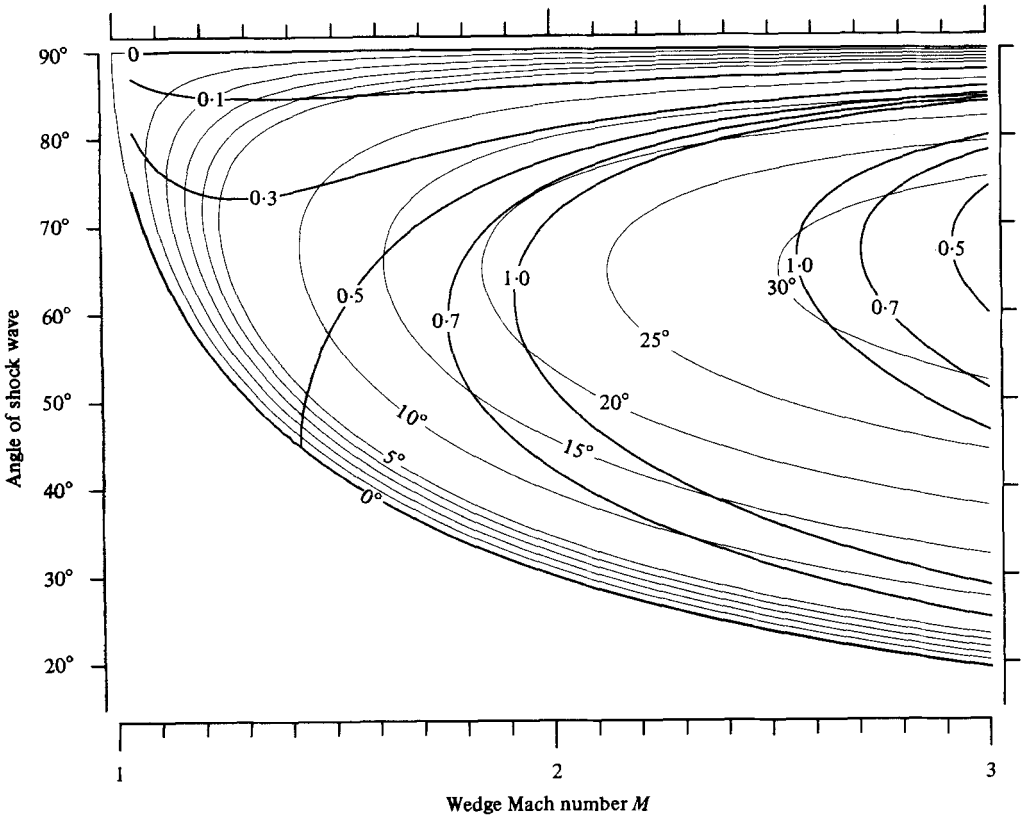

FIGURE 10. The wave amplitude, within the Mach wave region, due to the surface-monopole source, expressed as a fraction of the real amplitude $\Delta\rho$, (thick contours); and the shock-wave angle β, plotted for constant wedge angle α, (thin contours) as a function of the Mach number M.

for the scattered wave. The series expansion for the step wave does not converge in the familiar sense. Generally the first-order scattering contributes

$$\tau \frac{\partial p}{\partial t}(x+ct), \tag{8.3}$$

to the incident wave $p(x+ct)$, where τ is the displacement in arrival time arising from the past variations in phase speed.

The model problems discussed involve constant-amplitude waves, and the non-linear relationship between amplitude and phase speed has been avoided. But the one-dimensional piston-problem can be extended easily to include the case of simple-wave generation by a moving piston. The equations of mass and momentum conservation can be combined and written in characteristic form

$$\left(\frac{\partial}{\partial t}+(u\pm c)\frac{\partial}{\partial x}\right)\left(\int\frac{c(\rho)\,d\rho}{\rho}\pm u\right)=0. \tag{8.4}$$

This shows that the quantities $\int\rho^{-1}c(\rho)\,d\rho\pm u$ are constant on the characteristics $dx/dt = u\pm c$. Restricting the fluid to a perfect gas gives

$$\int\frac{c(\rho)\,d\rho}{\rho}=\frac{2c}{\gamma-1}. \tag{8.5}$$

If the fluid lying in the region $x > 0$ is at rest prior to the motion of the piston, then the characteristics $dx/dt = u + c$ extend into undisturbed fluid where $u = 0$, and $c = c_0$. On all these characteristics, therefore, $\int \rho^{-1} c(\rho)\, d\rho - u$ takes the value $2c_0/(\gamma - 1)$, and so the value of c on these characteristics is given by

$$\frac{2c}{\gamma - 1} = \frac{2c_0}{\gamma - 1} + u.$$

Where these characteristics meet the piston, the fluid velocity u is that of the piston V and so the value of $\int \rho^{-1} c(\rho)\, d\rho$ is $2c_0/(\gamma - 1) + V$. On the characteristics $dx/dt = u + c$, therefore,

$$\int \frac{c(\rho)\, d\rho}{\rho} + u = \frac{2c_0}{\gamma - 1} + 2V = \frac{2c}{\gamma - 1} + V. \tag{8.6}$$

Consequently

$$\left(\frac{\partial}{\partial t} + (u + c)\frac{\partial}{\partial x}\right) u = \left(\frac{\partial}{\partial t} + (c_0 + \tfrac{1}{2}(\gamma + 1)\, u)\frac{\partial}{\partial x}\right) u = 0. \tag{8.7}$$

This is a travelling-wave equation with an amplitude-dependent phase speed

$$c_0 + \tfrac{1}{2}(\gamma + 1)\, u.$$

The phase speed can if desired be adjusted to some constant $c_0 + \frac{1}{2}(\gamma + 1)\, v$, say, but only at the expense of introducing an inhomogeneity or source term.

The wave equation then takes the form

$$\left(\frac{\partial}{\partial t} + (c_0 + \tfrac{1}{2}(\gamma + 1)\, v)\frac{\partial}{\partial x}\right) u = \frac{\partial}{\partial x}\left(-\tfrac{1}{4}(\gamma + 1)\,(u - v)^2\right). \tag{8.8}$$

The amplitude-dependent wave is now described by a superposition of constant-speed wavelets driven by a nonlinear source term. Only when the correct phase speed $c_0 + \frac{1}{2}(\gamma + 1)\, u$, rather than $c_0 + \frac{1}{2}(\gamma + 1)\, v$, is chosen does the equation become source-free. Writing (8.8) as

$$\frac{D}{Dt}(u) = \frac{\partial}{\partial x}\left(-\tfrac{1}{4}(\gamma + 1)\,(u - v)^2\right) \tag{8.9}$$

enables it to be written in integral form

$$u(x_0 + (c_0 + \tfrac{1}{2}(\gamma + 1)\, v)\, t, t) = u_s - \int_{t_0}^{t} \tfrac{1}{4}(\gamma + 1)\frac{\partial}{\partial x}((u - v)^2)\Big|_{x = x_0 - (c_0 + \frac{1}{2}(\gamma + 1)v)(t - \tau)} d\tau, \tag{8.10}$$

where u_s is the surface velocity at the time t_0 when the wavelet left the surface. Additionally, the effect of a moving boundary, generating the wave say, can be incorporated to give inhomogeneous terms at the boundary and within the wave:

$$\frac{D}{Dt}(Hu) = \{\tfrac{1}{4}(\gamma + 1)\,(u - v)^2 - \tfrac{1}{2}(\gamma - 1)\, u(u - v) + uc_0 + \tfrac{1}{2}(\gamma - 1)\, u^2\} \times \frac{\partial H}{\partial x} - \frac{\partial}{\partial x}\{\tfrac{1}{4}(\gamma + 1)(u - v)^2 H\} \tag{8.11}$$

The choice $u = v$ eliminates the volume sources and some of the surface sources. The remaining surface terms disappear when either the boundary stops, or moves with

speed $-2c_0/(\gamma-1)$ to rarefy the medium. In the latter case (8.10) gives only the trivial result, the velocity at the bounding surface. The optimal form of the analogy in this one-dimensional case gives therefore the velocity field as $u = u_s$ at the correct time, i.e.

$$u(\mathbf{x}, t) = u_s(t - x/(c_0 + \tfrac{1}{2}(\gamma+1)\,u)). \tag{8.12}$$

The velocity wave is expressible in either homogeneous or inhomogeneous form; the latter gives a constant phase speed and the former an amplitude-dependent speed. A non-zero quadrupole distribution indicates a disparity between the physical phase speed and the imposed phase speed. This observation suggests that nonlinear flow effects, or quadrupoles, in irrotational flows amount to little more than a phase shift, and lead one to conclude that those quadrupoles are more reasonably thought of as 'wave-positioning' devices than they are wave generators. This view is consistent with Howe's (1975) analogy in which the acoustic sources in fluid flows are identified as requiring vorticity or entropy production. However both that analogy and these examples deal only with flows that are steady or quasisteady.

9. Conclusions

The two model flows illustrating the acoustic analogy indicate that the quadrupole source of (2.1) is very significant for highly disturbed flows. It is the dominant source for the high-subsonic-speed piston, for the transonic-speed thin wedge ($\alpha < 5°$), and also for the high-supersonic-speed wedge. But the quadrupole is the least significant source for weakly disturbed flows, being negligible for the low-speed piston flow and for thin wedges moving in the speed range $1{\cdot}3 < M < 1{\cdot}9$. This concurs with Hanson & Fink (1978), where only quadrupoles in the transonic speed range are appreciable.

But the role of the quadrupole term in these flows appears to be to re-position a surface-generated disturbance. This is made evident by adapting the phase speed of the analogy to match that of the flow, and it can easily be demonstrated for the wedge by using $c = V\sin\beta$ in (7.1) to make $\mu = \beta$. Changing the phase speed alters only the quadrupole source which can, in these problems, be eliminated altogether by selecting a particular phase speed for the acoustic analogy.

The presence of a shock produces a source term whose field is generally weak except at the transonic condition. This supports the impression that shocks should not be regarded as sources of waves in the acoustic analogy.

The boundary to the quadrupole source produces, in these cases, a high-amplitude field that is largely cancelled by an associated high-amplitude dipole field. The analogy of (2.1) does not appear helpful, since the separate fields of the sources, although individually large, interfere significantly, and the final field cannot be approximated usefully from a sub-set of the sources. This is in contradistinction to Hanson & Fink (1978) and Yu & Schmitz (1980), where for subsonic rotors, as opposed to the supersonic surfaces treated here, there is little destructive interference between the component fields.

Finally, it is shown that a linear approximation to the dipole strength underestimates the field to the extent of 100 % and more for high-transonic-speed thin wedges and this may be of importance to the design of computational models based on (2.1).

This work, part of a research programme at Cambridge University now supported by Rolls-Royce Limited, was started while the author was in receipt of an S.R.C. studentship. The support of both is gratefully acknowledged. The author is also deeply indebted to his research supervisor Professor J. E. Ffowcs Williams for valuable suggestions and patient guidance.

REFERENCES

BOXWELL, D. A., YU, Y. H. & SCHMITZ, F. H. 1978 Hovering impulsive noise: some measured and calculated results. *N.A.S.A. Conf. Proc.* CP2052.

BRYAN, G. H. & LAMB, H. 1920 The acoustics of moving sources with application to airscrews. *Aero. Res. Comm. Rep. & Mem.* no. 684.

CROW, S. C. 1969 Distortion of sonic bangs by atmospheric turbulence. *J. Fluid Mech.* **37**, 529–563.

CURLE, N. 1955 The influence of solid boundaries upon aerodynamic sound. *Proc. R. Soc. Lond.* A **231**, 505–514.

FARASSAT, F. 1975 Theory of noise generation from moving bodies with an application to helicopter rotors. *N.A.S.A. Tech. Rep.* R-451.

FFOWCS WILLIAMS, J. E. 1976 The theoretical modelling of aerodynamic noise. *Proc. Indian Acad. Sci.* **1**, 57–72.

FFOWCS WILLIAMS, J. E. 1979 On the role of quadrupole source terms generated by moving bodies. *A.I.A.A. Paper* no. 79-0576.

FFOWCS WILLIAMS, J. E. & HAWKINGS, D. L. 1969 Sound generation by turbulence and surfaces in arbitrary motion. *Proc. R. Soc. Lond.* A **264**, 321–342.

GARRICK, I. E. & WATKINS, C. E. 1954 A theoretical study of the effect of forward speed on the free-space sound-pressure field around propellers. *N.A.C.A. Tech. Memo.* no. 1198.

GUTIN, L. 1940 On the sound field of a rotating propeller. *N.A.C.A. Tech. Memo.* no. 1195.

HANSON, D. B. & FINK, M. R. 1978 The importance of quadrupole sources in prediction of transonic tip speed propeller noise. *J. Sound Vib.* **62**, 19–38.

HOWE, M. S. 1975 Contributions to the theory of aerodynamic sound. *J. Fluid Mech.* **71**, 625–673.

LIGHTHILL, M. J. 1952 On sound generated aerodynamically. I. General theory. *Proc. R. Soc. Lond.* A **211**, 546–587.

LIGHTHILL, M. J. 1953 On the energy scattered from the interaction of turbulence with sound or shock waves. *Proc. Camb. Phil. Soc.* **49**, 531–551.

LYNAM, E. J. H. & WEBB, H. A. 1920 The emission of sound by airscrews. *Aero. Res. Comm. Rep. & Mem.* no. 792.

YU, Y. H. & SCHMITZ, F. H. 1980 High-speed rotor noise and transonic aerodynamics. *A.I.A.A. Paper* no. 80-1009.